J. Phys. B: At. Mol. Opt. Phys. **44** (2011) 195601 (8pp) doi:10.1088/0953-4075/44/19/195601

High-order harmonic generation from coherently excited molecules

Jun Bao, Wenbo Chen, Zengxiu Zhao[1] and Jianmin Yuan

Department of Physics, National University of Defense Technology, Changsha 410073, People's Republic of China

E-mail: zhao.zengxiu@gmail.com

Received 13 July 2011, in final form 8 August 2011
Published 1 Septemter 2011
Online at stacks.iop.org/JPhysB/44/195601

Abstract

High-order harmonic generation (HHG) from electronically excited molecules exposed to single-cycle laser pulses is investigated. H_2^+ ions are used as an example under the condition that they are prepared in a coherent superposition of the two lowest lying states. We show that the populated excited state can be used to gate the ionization and the HHG processes. The HHG yields are found dependent on the coherent phase and the carrier-envelope phase of the laser pulse, providing the possibility of monitoring electron localization dynamics. We further demonstrate that the presence of multi-path recombinations leads to interference in harmonic yields enabling the determination of harmonic chirp.

(Some figures in this article are in colour only in the electronic version)

1. Introduction

High-order harmonic generation (HHG) from atoms interacting with intense few-cycle laser pulses opens the door to generate attosecond (as) pulses [1, 2]. Recently, the duration of such XUV pulses has been reduced to 130 as [3] and 80 as [4], approaching the Kepler period of a classical electron revolving around the proton (150 as). Electronic motions inside atoms, molecules and solids can be traced, probed and even steered with attosecond resolution in real time [5–7], advancing the study on ultrafast dynamic processes (see reviews [8–12]).

A three-step model [13–15] has been introduced to interpret HHG. A free electron wavepacket is formed through tunnel ionization of the atom, part of which is driven back and forth in the vicinity of the atomic core by the time-varying electric field. The interference between the free electron wavepacket and the bound part of the wavefunction gives rapid oscillating electron current and high-order harmonic radiation is emitted in correspondence to photo recombination. According to this rescattering model, radiation burst is generated each half-cycle forming a train of XUV pulses. In order to get isolated single attosecond pulses, first, the emission process, or the underlying ultrafast electron dynamics, has to be controlled. By reducing the time duration of the driving laser pulse to a few cycles [16] or even a single cycle [4, 17, 18], it is possible to make only one dominant recombination event occur [16] because tunnelling ionization is extremely sensitive to electric fields [19]. Secondly, the carrier-envelope phase (CEP) of the driving pulse needs to be stabilized to spectrally filter the harmonics [16]. Other proposals involve polarization gating [20], two-colour optical gating [21] or using a resonant harmonics [22]. Recently, it has been proposed to combine the former two into a double optical gating (DOG) setup that has the advantage of generating as pulses with 20 fs laser pulses [23, 24].

Controlling atomic states, on the other hand, provides a different approach to manipulate HHG processes [25–27]. HHG from coherently excited atoms have been studied in previous works [28, 29, 31], but focused on the enhancement of HHG efficiency and extension of harmonic cut-off energy. We have recently studied the harmonic generation from a vibrational excited molecules and showed that the HHG yielding efficiency follows the evolution of nuclear wavepacket [30]. In this work, we examine the interference of HHG processes when molecules are prepared in a coherent superposition of electronic states.

It seems that preparing the atom in a coherent state only leads to the coherent superposition of individual time-dependent wavefunctions and can hardly make any change in the physics. However, this linearity is only for the electron wavefunctions and not for the external light field. As a

[1] Author to whom correspondence should be addressed.

consequence, all of the resulting physical quantities can be obtained from the coherent superposition of independently time-evolved wavefunctions from each individual initial state. The HHG, on the other hand, are highly nonlinear processes and are very sensitive to the coherent superposition of the electronic states. It was pointed out that the double plateau structure appeared in the HHG from coherently excited atoms [31]. The existence of populations on the ground state (GS) and the excited state (ES) provides additional pathways for harmonic generation. The coherent phase is important for HHG in the higher plateau region even for long pulses [32]. For few-cycle or single-cycle pulses, the relative phase is expected to make more effects on HHG in the pathway that the electron leaves from one bound state and recombines to the other. In this study, we show that by using a single-cycle laser pulse, the coherently excited molecules can be used as an 'atom grating' for HHG. The interference between different recombination paths enables the determination of harmonic chirp which is crucial in generating even shorter attosecond pulses.

When diatomic molecules are electronically excited, the electron population jumps back and forth between the two nuclei and is localized temporally. Electron localization plays an important role in chemical bond-breaking [33], molecule forming and dissociating [34], charge transfer collision and charge resonance enhanced ionization (CREI) [35, 36], to name a few. With the availability of attosecond pulses, it is possible to observe electron population dynamics [37, 38] and control electron localization in molecules [39]. On the other hand, as IR laser pulses are compressed to several femtoseconds, electron localization and dissociating pathways [40–42] can be controlled without involving attosecond pulses. Information on electron localization is usually obtained from photoelectron spectroscopy or fragmentation. Since HHG is a highly nonlinear process, we would expect that the harmonic yield is sensitive to the localization of electron population. Recently, it has been demonstrated experimentally that HHG provides a high sensitivity tool of probing ES dynamics [43, 44]. Simultaneous measurement of HHG and ion yields from dissociating Br_2 molecules shows that interference occurs for harmonics generated from the ground and the ES, permitting sensitive detection of chemical changes. Our motivation of this work is therefore two-fold: (i) how to probe ultrafast electronic dynamics with HHG by using CEP-stabilized laser pulses; and (ii) how to control and measure HHG by coherent control of molecular states.

The paper is organized as follows. In section 2, we first study the dynamics of GS molecules and excited molecules in single-cycle laser pulses. In section 3, we discuss the HHG from coherently excited molecules and relate the electron localization to the CEPs of laser pulses. In section 4, we propose a method to determine the chirp of the harmonics. Finally, a short summary and conclusion is given. Atomic units ($\hbar = e = m_e = 4\pi\varepsilon_0 = 1$) are used unless stated otherwise.

2. Dynamics of GS and ES molecules

In this section, we examine the different responses of molecules prepared initially in either GS or the first ES to single-cycle laser pulses at various of CEPs. A one-dimensional model H_2^+ is considered with nuclear separation fixed at 2 au. The Coulomb potential from either nucleus is softened to remove the non-physical singularity for 1D space. The soft-core parameter is chosen as 1.44 [45] to yield the correct electronic GS energy of real H_2^+ molecule. The ionization energies of GS and ES are found to be $I_1 = 1.11$ and $I_2 = 0.73$ au, respectively. The time-dependent Schrödinger equation is numerically solved using the split-operator method with details presented in [30]. The result has been found converged with a box size of 500 au, using 163 84 grid points.

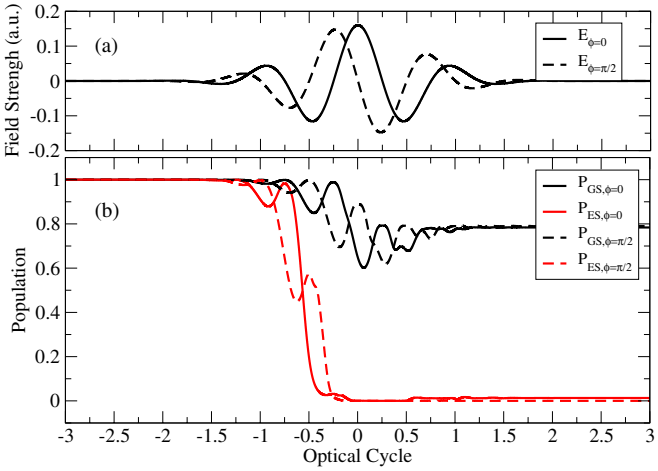

Figure 1. (a) Instantaneous electric fields for CEPs of 0 (solid lines) and $\frac{\pi}{2}$ (dashed lines). (b) Population in the initial states for molecules prepared in the electronic ground state (black lines) and the first excited state (red lines) subjected to a laser pulse with CEPs of 0 (solid lines) or $\frac{\pi}{2}$ (dashed lines), respectively.

The laser pulse has a Gaussian intensity profile with full width at half maximum (FWHM) intensity of one optical cycle (2.67 fs) at wavelength of 800 nm. For such short pulses, the CEPs make big differences on the instantaneous electric fields as plotted in figure 1(a) for CEP of 0 and $\pi/2$ radian. The CEP will be denoted by ϕ in the following. Let us first consider the ionization of GS H_2^+ molecules in the laser intensity of 9×10^{14} W cm^{-2}. It can be seen from figure 1(b) that the survived population alters little when the CEP is changed from 0 to $\pi/2$ radian. But in comparison the instantaneous population of the GS shows nearly out of phase $\frac{\pi}{2}$ oscillations suggesting that the laser-induced population dynamics, as well as HHG processes, are very sensitive to the CEPs. At $\phi = 0$, the maximum laser field coincides with the maximum of intensity envelope. The harmonic spectra from the GS molecule exhibit two cut-off energies as shown in figure 2. The lower cut-off energy (∼70th order) can be attributed to the rescattering in the neighbouring cycle of the envelope center, while the larger cut-off energy (∼130th order) is caused by the rescattering of electron driven by the peak field. In the case of $\phi = \frac{\pi}{2}$, there exist two peak fields at the same magnitude; therefore, the HHG from recombinations in the two consecutive cycles result in the same cut-off energy. It is hence evident that the step-like behaviour of plateaus reflects subcycle dynamics;

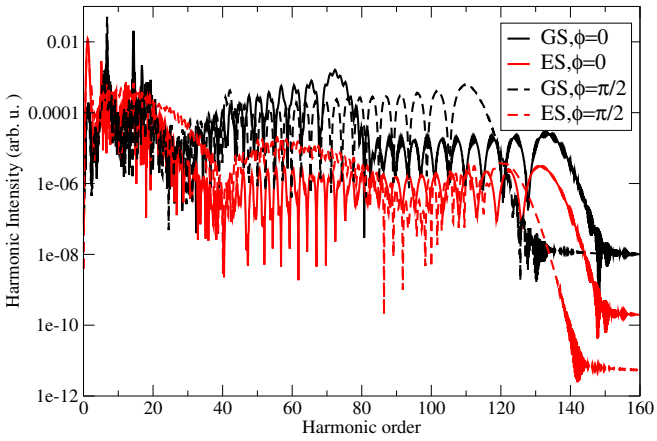

Figure 2. Harmonic spectra from molecules prepared in the electronic ground state and the first excited state subject to laser pulses of CEP 0 and $\frac{\pi}{2}$.

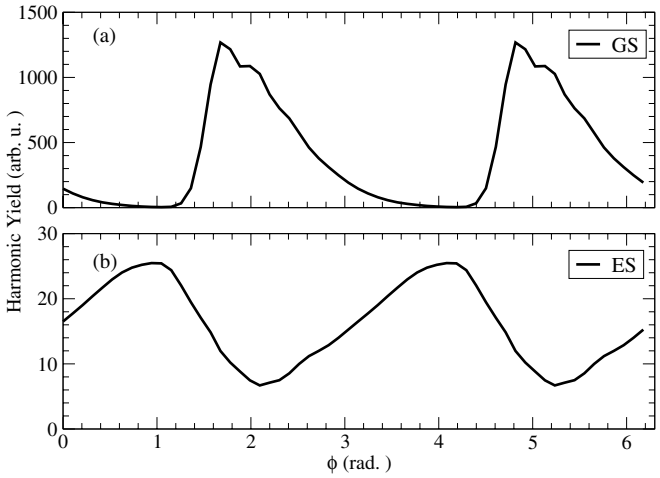

Figure 3. Integrated spectral yields over harmonic order of 110 and 150 versus CEPs of the laser pulse from molecules prepared in (a) the electronic ground state and (b) the first excited state.

however, it can only be resolved if the duration of CEP-stabilized laser pulse approaches a few cycles or a single cycle [7]. Note that the dip structure at the harmonic order of H25 exhibited in the spectra is caused by the destructive two-center interference in the energy-dependent recombination dipole moment [45].

For the ES molecule, the population of the ES is quickly depleted before the field reaches its maximum as shown in figure 1(b) because of the smaller ionization energy. In comparison, about 80% of GS population survives after the pulse is turned off. A direct consequence of this different behaviour is that the HHG intensity is much lower for ES as shown in figure 2 because the returning electron sees less population left in the initial state. Because of the different symmetry of the ES from the GS, the position of minimum shifts to H39 as seen in figure 2.

In order to examine the dependence of harmonic yields on CEPs quantitatively, we integrate the harmonics spectra in a window from order H110 to H150 as shown in figure 3. For the GS, the yield takes a maximum at CEP $\phi = \pi/2$ which is not a surprise since there are two sub-peaks of the laser field that contribute. However, for the ES, the harmonic yield takes a maximum at CEP $\phi = 0.3\pi$, mainly because of the depletion of the excited state before the field reaches its maximum.

3. Harmonic generation from coherently excited molecules

Now we turn to HHG from molecules pre-excited to coherent superpositions of the GS and ES which can be achieved by pumping molecules with the seventh harmonic of 800 nm infrared laser.

The molecular wavefunction after excitation can be written as $\psi(t_0) = a_1\phi_G + a_2\phi_E$ where the eigenfunctions of the GS and ES are denoted by ϕ_G and ϕ_E, and the corresponding probability amplitudes are given by a_1 and a_2, respectively. The relative phase of a_1 and a_2 varies as $\theta = \Delta E t_0$ when the molecules are evolving freely, where $\Delta E = I_1 - I_2$ is the difference between the ionization potentials of the two states, i.e. the excitation energy from the GS to the ES.

Because the wavefunctions of GS and ES have different symmetry under electron coordinate inversion, the electron density of the free-evolving molecule shows classical behaviour: the population density is oscillating between the two nuclei [37, 38]. The oscillation period is inversely proportional to ΔE and is about 200 as in the present study. Observing such rapid oscillations usually involves employing attoseond pulses [38]. But as shown in the experiments of determining attosecond pulse durations [4] and tunnelling time [7], phase-stabilized few-cycle laser pulses have the capability of being applied to probe attosecond dynamics thanks to the nonlinearity of tunnel ionization. We will show next that how the localization dynamics is probed and how the ES can be used to gate the HHG.

Subjected to a probe laser pulse at time t_0, the time-dependent wavefunction of the molecule is given by

$$\Psi(t) = a_1 U(t, t_0)\phi_G + a_2 U(t, t_0)\phi_E \equiv a_1\psi_G + a_2\psi_E, \quad (1)$$

where $U(t, t_0)$ is the evolution operator and a_1 and a_2 have a phase difference θ to which we will refer as the initial coherent phase.

The induced dipole moment of the molecule driven by the laser pulse can be expressed as

$$D(t) = |a_1|^2 d_1 + |a_2|^2 d_2 + \{a_1^* a_2 d_3 + \text{c.c}\}, \quad (2)$$

where

$$d_1(t) = \langle\psi_G|\, x\, |\psi_G\rangle \quad (3)$$

$$d_2(t) = \langle\psi_E|\, x\, |\psi_E\rangle \quad (4)$$

$$d_3(t) = \langle\psi_G|\, x\, |\psi_E\rangle\,. \quad (5)$$

The emitted harmonic spectra can be obtained by Fourier transforming

$$I_\omega = \left| \int \mathrm{e}^{\mathrm{i}\omega t} (|a_1|^2 d_1 + |a_2|^2 d_2 + d_x)\, \mathrm{d}t \right|^2, \quad (6)$$

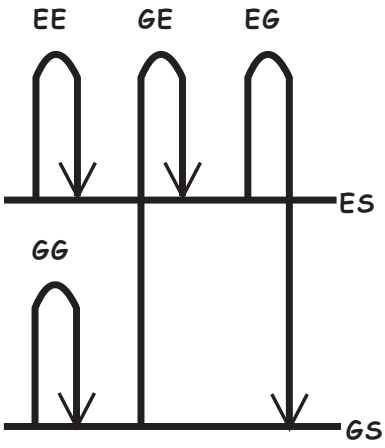

Figure 4. Illustration of HHG pathways. When molecules are coherently populated in two states indicated by GS and ES, there are four possible paths contributing to HHG labelled based on which states the electron is released and into which states it recombines.

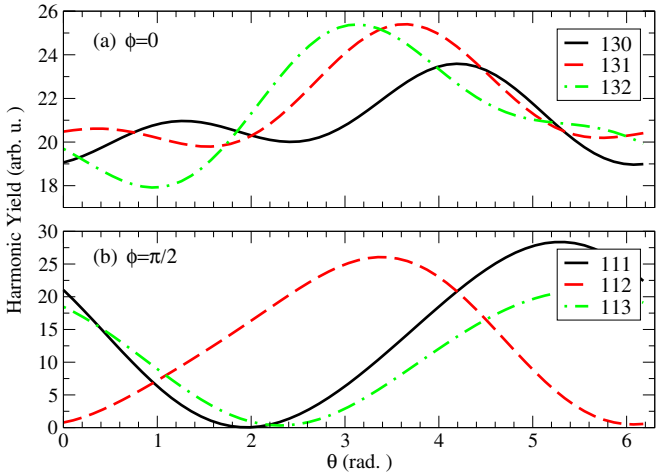

Figure 5. Variation of harmonic intensity with the initial phase θ for laser CEP of (a) $\phi = 0$ and (b) $\phi = \frac{\pi}{2}$ for the given harmonic orders labelled. The molecules are prepared in a coherent superposition of the ground state and the first excited state with a population ratio of 1 : 1.

where we have introduced

$$d_x = a_1^* a_2 d_3 + \text{c.c.} \tag{7}$$

It is clear that equations (3) and (4) give the HHG from molecules initially in the GS and ES, respectively. However, when the molecules are prepared in a coherent superposition, an interference term given by equation (7) arises as an natural consequence of the quantum coherence.

Based on the rescattering model, there are four pathways of harmonic emission because the electron can be released from and recombines into either the GS or the ES. The four pathways are denoted by GG, EE, GE, EG as illustrated in figure 4, where GE, for example, represents an electron released from the GS and recombines into the ES. The total harmonic yield therefore depends on the interference of the different pathways which cannot be trivially considered because the HHG is a highly nonlinear process. By varying θ, the relative phase of a_1 and a_2, the phase of each path can be controlled and the interference effects on the harmonic yields can be monitored. Note that the intensity of the resonant transition from the ES to the GS is mainly determined by $|a_1^* a_2|$ and is independent of θ as shown in [28].

In figure 5, we examine the θ dependence of harmonic yields by taking $|a_1|^2 : |a_2|^2 = 1 : 1$. Consider the emission of a photon of energy ω. Following the spirit of strong field approximation [15] and keeping only the relevant terms involved in equation (7), the time-dependent wavefunctions $\psi_G(t)$ and $\psi_E(t)$ can be written as $b_G(t)\phi_G\, \mathrm{e}^{-\mathrm{i}E_G t} + \phi_c\, \mathrm{e}^{-\mathrm{i}(E_E+\omega)t}$ and $b_E(t)\phi_E\, \mathrm{e}^{-\mathrm{i}E_E t} + \phi_c\, \mathrm{e}^{-\mathrm{i}(E_G+\omega)t}$, where ϕ_c represents the continuum state responsible for the emission of a photon energy of ω upon recombination. In reality, ϕ_c is a time-dependent wavepacket, and significant emission occurs when it approaches the molecular core. Here, we assume it is slowly oscillating in time compared to the harmonic phase ωt. After pulling out the term of $\mathrm{e}^{-\mathrm{i}\omega t}$, the remaining part in equation (7) is

$$a_1^* a_2 \langle \phi_G | x | \phi_c \rangle b_G^* + a_1 a_2^* \langle \phi_E | x | \phi_c \rangle b_E^*, \tag{8}$$

where the first and the second terms are referred to as EG and GE paths, respectively. It is now evident that the EG path is weighted by the remaining population on the GS and with theta dependence of $\mathrm{e}^{-\mathrm{i}\theta}$, while the GE path is weighted by $|b_E|^2$ and depends on θ as $\mathrm{e}^{\mathrm{i}\theta}$. The contribution from the GE path will vanish if the population of the ES is depleted at the instant of recombination. Explicitly writing down the θ dependence of equation (6), we have

$$I_\omega(\theta) \sim |w_1 + w_2\, \mathrm{e}^{-\mathrm{i}\theta} + w_3\, \mathrm{e}^{\mathrm{i}\theta}|^2, \tag{9}$$

where the weight factors w_i, $i = 1, 2, 3$, are dependent of the harmonic order and laser parameters.

In the case of $\phi = 0$, both of the GE and EG paths contribute, and the spectra vary as $\cos 2\theta$, while for $\phi = \frac{\pi}{2}$, the population in the ES is almost completely depleted as shown in figure 1; therefore, the contribution of the path GE vanishes, giving rise to $\cos\theta$ dependence. Other harmonics examined show a similar behaviour. The fast depletion of the ES determines how the ES contributes to HHG and therefore can be used as a gate to control HHG processes. Next we show that this gate can be used to probe the localization dynamics of the electron.

Due to the coherent superposition of the GS and ES, the recombining electron finds the bound part of the wavefunction different when driven by laser fields with CEPs differed by π. The broken left and right symmetry causes unequal HHG yields reflecting the localization of the electron population as will be demonstrated below. When ϕ is changed by π, d_1 and d_2 change signs while d_3 remains the same. At a given photon energy, the difference of harmonic intensity, denoted as $\Delta I(\omega) = I_\phi(\omega) - I_{\phi+\pi}(\omega)$, is given by

$$\Delta I(\omega) = 2[|a_1|^2 \tilde{d}_1(\omega) + |a_2|^2 \tilde{d}_2(\omega)]\tilde{d}_3^*(\omega) + \text{c.c.}, \tag{10}$$

where $\tilde{d}(\omega)$ represents the Fourier transformation of $d(t)$. Considering the harmonic yields within a spectral window from ω_1 to ω_2, the total yield difference is given by

$$\Delta S = \int_{\omega_1}^{\omega_2} \Delta I(\omega)\, \mathrm{d}\omega. \tag{11}$$

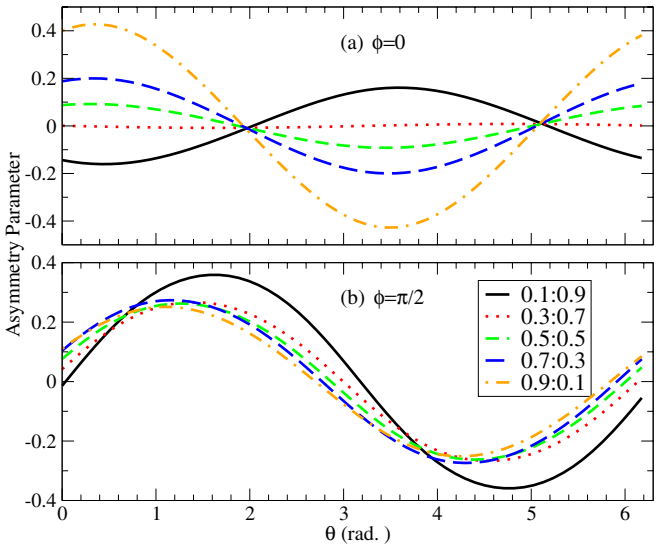

Figure 6. The asymmetry parameter versus phase θ for CEPs (a) $\phi = 0$ and (b) $\phi = \frac{\pi}{2}$. Different population ratios of the GS to the ES are labelled $|a_1|^2 : |a_2|^2$.

We define the asymmetry parameter as the total yield difference divided by the sum of the two yields S_1 and S_2 at CEP ϕ and $\phi + \pi$:

$$\gamma = \frac{\Delta S}{S_1 + S_2}. \tag{12}$$

Clearly, the asymmetry parameter is a function of θ and ϕ. In figure 6, we present the θ dependence of γ for CEP of 0 and $\frac{\pi}{2}$ with different initial states. The spectral window is again chosen as a harmonic order (H110–H150) as it was previously. It can be seen that the asymmetry parameter oscillates with the initial phase θ periodically with a period of 2π for all of the different relative population configurations. The dependence on the initial phase implies that the asymmetry of the HHG yield varies with time in frequency of ΔE which is related to the localization dynamics of the electron in the molecule. This extreme sensitivity to the initial phase has nothing to do with a short pulse and everything to do with the phase stabilization of the laser pulse which allows a control of the sub-cycle dynamics such as ionization and recombination on a much finer time scale.

It can be seen in figure 6 that the maximum magnitude of γ varies with the population configuration at $\phi = 0$, while it shows little variation at $\phi = \frac{\pi}{2}$. The reason is that the ratio of $|d_1|$ to $|d_2|$ is different for the two CEPs. At $\phi = \frac{\pi}{2}$, the ratio is about 8:1 such that the asymmetry hardly changes with the relative population. In order to observe the initial phase dependence of the asymmetry harmonic yields, one could coherently excite the molecules with a pump pulse and then probe at a different time delay by measuring the corresponding HHG yield. But with CEP stabilized probing laser pulses, one can determine this dependence by varying the CEP continuously without changing the time delay. Since the carrier frequency of the probing pulse is about 1/6 of the oscillating frequency of the electron density, one would expect that the asymmetry of the HHG yield would oscillate six times faster with the CEP than with the initial phase.

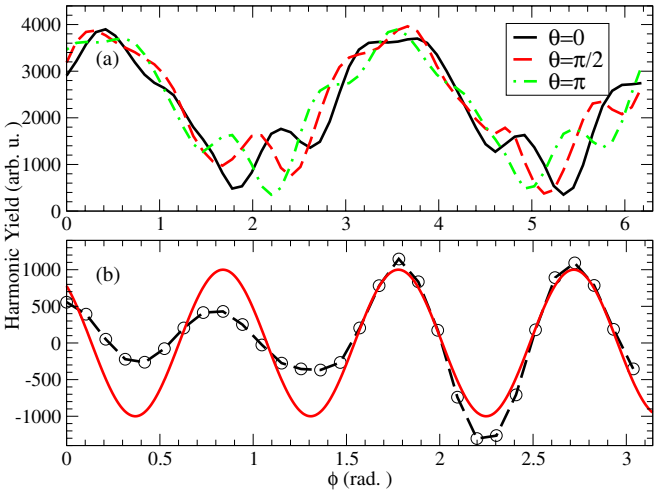

Figure 7. (a) Variation of harmonic yields with CEP for given initial phases θ; (b) difference of harmonic yields between laser CEP ϕ and $\phi + \pi$ for $\theta = 0$.

In figure 7(a), we show the variation of HHG yields with CEP at given initial phases. The relative population of the GS and ES is fixed at 0.9:0.1. The yield is modulated with varying CEP. Note that shifting θ by π is equivalent to varying CEP by π. If we examine that the difference of the HHG yield between the CEP differed by π, the oscillation can be clearly seen as shown by the dotted lines in figure 7(b), which can be fitted by

$$\cos\left(\frac{\Delta E}{\omega_0}\right) = \cos(6.6841\phi) \tag{13}$$

shown by the solid lines. Therefore, we demonstrate that the interference between the different HHG emission paths gives the asymmetry of HHG yields. Furthermore, the dependence of HHG on the coherent phase of the two molecular states can be monitored by controlling the CEP of the probing laser pulse.

In the above simulation, the nuclear separation is fixed. But in reality, the first excited electronic state is dissociated with nuclear motion governed by the Born–Oppenheimer potential curve of the excited electronic state. As the ionization energy varies little in comparison with the Coulombic repulsive potential between the two nuclei, the latter can be used to estimate the dissociation dynamics. Starting with 2 au, the nuclear separation R is estimated to be 4 au after one optical cycle (2.7 fs). While the ionization energy of the first ES changes by 0.4 eV (based on our 1D calculation), the vertical excitation energy changes from 0.38 to 0.13 au. Therefore, one might think that the monitoring of the bound state dynamics will be blurred by the varying excitation energy. But, in fact, the nuclear separation of the GS peaks at the equilibrium distance and the ground nuclear wavepacket stays in the initial ground vibrational state (where we assume the molecule initially in the lowest vibration level). The excitation energy can still be approximated by the difference of the electronic energy of the first ES at each R and the GS energy at the equilibrium nuclear separation. Therefore, the scale of relevant energy is hardly modified by the dissociation

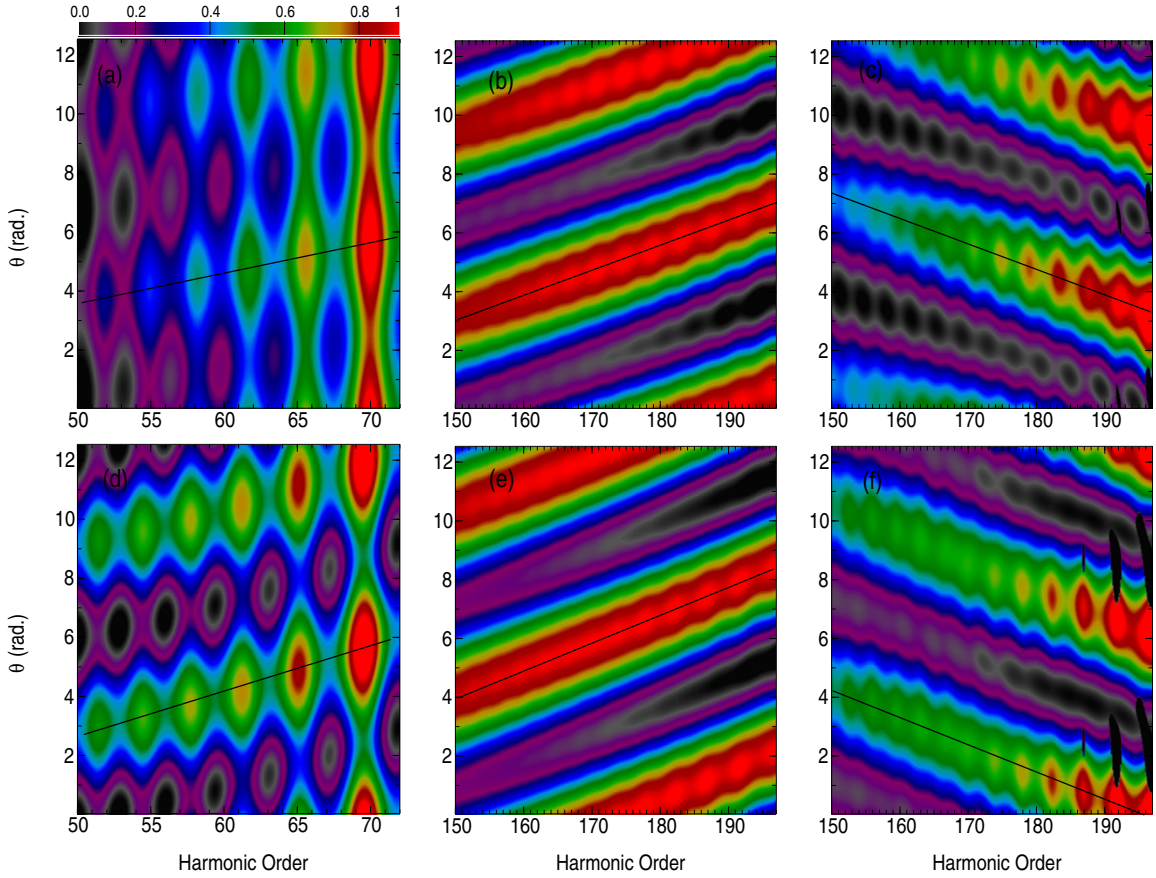

Figure 8. Contour plot of harmonic yield as a function of the harmonic order and the relative phase θ between the two states. The positions where HHG yield takes maximum form a straight line with slope encoding the chirp information of the harmonics. Note that the range of the phase is extended to 4π for better visualization. The intensity of yield is coded in red to black from high to low with the highest intensity normalized to 1. (a) 1D, $\omega_L = 800$ nm, short trajectory; (b) 1D, $\omega_L = 1600$ nm, short trajectory; (c) 1D, $\omega_L = 1600$ nm, long trajectory; (d)–(f) 2D simulations of (a)–(c) with the corresponding parameters. The laser intensities and the wavelet scaling parameters are $I = 5 \times 10^{14}$ W cm^{-2}, $\sigma = 45$ for 800 nm and $I = 2 \times 10^{14}$ W cm^{-2}, $\sigma = 90$ for 1600 nm, respectively.

of the ES. But the nuclear wavefunctions of the ES and the GS and their overlap does need to be considered in HHG processes for realistic investigation. The phase variation of the photo-recombination dipole moment with R, and the resulting interference between different pathways of HHG needs to be examined more carefully which will be addressed in future work.

4. Measuring the chirp of harmonics

The relative phase between the two coherent states varies with the time delay after it is pumped. The order-dependent harmonic intensity is hence a function of the relative phase. To resolve the contribution of a given trajectory of the HHG intensity, we employ the time–frequency analysis by means of wavelet transformation [46, 47]. The time profile $\mathcal{D}(\omega, \tau)$ of the acceleration dipole $d(t)$ is given by

$$\mathcal{D}(\omega, \tau) = \int [d(t) \times \sqrt{\omega} W(\omega t - \omega\tau)]\, \mathrm{d}t, \qquad (14)$$

with a Morlet mother wavelet $W(x) = (1/\sqrt{\sigma})\, \mathrm{e}^{\mathrm{i}x}\, \mathrm{e}^{-x^2/2\sigma^2}$, where the scaling parameter σ measures the width of the filtering window. For a given frequency ω, first, we identify the short (long) trajectory recombination from the maximum of time profile $|\mathcal{D}(\omega, \tau)|^2$ within each cycle; then the sum of these maxima over cycles is used to represent the total radiation intensity of short (long) trajectory of frequency ω. In such a way, we mimic the phase-matching process of macroscopic HHG.

In order to eliminate the two HHG paths that start with ionization of the GS, we choose a lower laser intensity at 5×10^{14} W cm^{-2} such that the ionization from the GS is negligible. The two remaining HHG pathways are EG and EE starting with ionization of the ES and ending into either the GS or the ES upon recombination. For given harmonic energy, electrons in the two pathways have returning energy differed by ΔE. According to the rescattering theory, the excursion time is roughly linearly proportional to the returning energy [48, 49]. Therefore, the phase difference of the two paths due to recombination into the GS and ES in the generation of the Nth harmonic can be approximated by [50]

$$\Delta\phi(\omega_N) \sim \tau_N \Delta E + \theta, \qquad (15)$$

where τ_N is the excursion time of electron recombining to its original state in the rescattering process. We have introduced the phase difference θ between the two molecular states that

does not come into play in the generation of harmonics from mixed gases [50]. Approximating the *N*th harmonic photon energy by the returning energy, the recursion time defines the chirp of harmonics through

$$\tau_N = \pm C\omega_N, \tag{16}$$

where C denotes the chirp of the harmonics and takes a positive (negative) value for short (long) trajectories [48, 49]. Finally, the phase difference of the two paths can be approximated by

$$\Delta\phi(\omega_N) \sim \pm CN\omega\Delta E + \theta. \tag{17}$$

Based on equation (17), the intensity of the *N*th harmonic takes a maximum value when the phase difference is integer multiples of 2π such that constructive interference (CI) occurs. Figure 8 shows the contour plot of harmonic yield as a function of the harmonic order and the coherent phase θ between the two states. The positions of CI form a straight line with harmonic order against the coherent phase θ. The slope of this line can be used to determine the chirp parameter C, which is estimated to be 4.1 as eV^{-1} in figure 8(a), 6.9 as eV^{-1} in figure 8(b) and -6.9 as eV^{-1} in figure 8(c) in our simulation. Here, different intensities and wavelengths are examined.

So far, the simulation is limited to one-dimensional electronic motion. In order to show that the scheme of chirp determining is realistic, we perform calculations with electron moving in two dimensions that takes account of the transversal spreading of the electron wavepacket. As shown in figures 8(d)–(f), the two-dimensional calculations give similar chirp compared to one-dimensional calculations.

Compared to RABBIT methods of measuring attoseond pulse chirp [1, 48, 51], we see that both schemes take advantage of two-photon processes. However, in the RABBIT scheme, a harmonic photon and an infrared photon are absorbed simultaneously through ionization processes. But in our scheme, a photon is absorbed first to excite the molecule, and then a harmonic photon is emitted through HHG. In a way, it is similar to HHG from mixed gases proposed in [50] to make use of the ionization potential difference of the two atomic gases. However, in our scheme, the ionization potential difference is due to the recombination to two coherent atomic states. Therefore, it removes the possible difficulty of phase matching caused by different ionization rates from two different kinds of atoms.

5. Summary

We have studied HHG from coherently excited molecules using a hydrogen molecular ion as an example. The populated excited states allow multiple pathways of harmonic generation. The interference between different pathways has been demonstrated to be important in studying multielectron effects of CO_2 molecules [52] in intense laser fields. While no multielectron effects are involved in the present investigation, the coherent excitation leads to localization of electron population. By varying the coherent phase between the ground and the first excited states, we have shown that the yield of HHG can be used to monitor the bound state dynamics. Although limited by one-dimensional simulation the tomographic imaging of the excited electron orbital using HHG is not investigated in this work, we expect that HHG from coherently excited of molecules will help us better understand the excited states, especially in multi-electron systems.

We have shown that the sensitivity of tunnel ionization on binding potential and instantaneous electric field parameters enable us to control HHG in attosecond time scale by varying laser intensity, pulse duration and laser CEP. Particularly, the rapid depletion of the excited states turns into a pro of gating HHG pathways, by taking advantage of the fact that recombination requires populated bound states. We further show that HHG from pre-excited molecule is an alternative approach of the RABBIT method of measuring the chirp of harmonics. Because molecules are excited coherently, phase matching in macroscopic HHG from molecular gases can be achieved by locking the time delay between pumping and probing.

Finally, we have to point out that the nuclear motion is frozen in this work. The nuclear separation-dependent bound state dynamics and the corresponding harmonic generation process have been studied experimentally on neutral molecule Br_2 [43, 44]. In order to theoretically address this issue, it would be necessary to perform *ab initio* calculation including both electronic (more than one electron) and nuclear motions.

Acknowledgments

This work was supported by the National Natural Science Foundation of China under grant nos 10676039 and 10874245, the National Basic Research Program of China (973 Program) under grant no 2007CB815105, and the National High-Tech ICF Committee in China. Funding support (SKLLIM1107) from the State Key Laboratory of Laser Interaction with Matter is acknowledged.

References

[1] Paul P M, Toma E S, Breger P, Mullot G, Auge F, Balcou Ph, Muller H G and Agostini P 2001 Observation of a train of attosecond pulses from high harmonic generation *Science* **292** 1689

[2] Drescher M, Hentschel M, Kienberger R, Uiberacker M, Yakovlev V, Scrinzi A, Westerwalbesloh Th, Kleineberg U, Heinzmann U and Krausz F 2002 Time-resolved atomic inner-shell spectroscopy *Nature* **419** 803

[3] Sansone G *et al* 2006 Isolated single-cycle attosecond pulses *Science* **314** 443

[4] Goulielmakis E *et al* 2008 Single-cycle nonlinear optics *Science* **320** 1614

[5] Kienberger R *et al* 2002 Steering attosecond electron wave packets with light *Science* **297** 1144

[6] Kienberger R *et al* 2004 Atomic transient recorder *Nature* **427** 817

[7] Uiberacker M *et al* 2007 Attosecond real-time observation of electron tunnelling in atoms *Nature* **446** 627

[8] Brabec T and Krausz F 2000 Intense few-cycle laser fields: frontiers of nonlinear optics *Rev. Mod. Phys.* **72** 545

[9] Drescher M, Hentschel M, Kienberger R, Tempea G, Spielmann C, Reider G A, Corkum P B and Krausz F 2001 X-ray pulses approaching the attosecond frontier *Science* **291** 1923

[10] Agostini P and DiMauro L F 2004 The physics of attosecond light pulses *Rep. Prog. Phys.* **67** 813

[11] Scrinzi A, Ivanov M Yu, Kienberger R and Villeneuve D M 2006 Attosecond physics *J. Phys. B: At. Mol. Opt. Phys.* **39** R1

[12] Krausz F and Ivanov M 2009 Attosecond physics *Rev. Mod. Phys.* **81** 163

[13] Corkum P B 1993 Plasma perspective on strong-field multiphoton ionization *Phys. Rev. Lett.* **71** 1994

[14] Kulander K C, Schafer K J and Krause J L 1993 *Super Intense Laser Atom Physics* (*NATO Advanced Studies Institute, Series B: Physics* vol 316) ed B Piraux, A L'Huillier and K Rzazewski (New York: Plenum) p 95

[15] Lewenstein M, Balcou Ph, Ivanov M Yu, L'Huillier A and Corkum P B 1994 Theory of high-harmonic generation by low frequency laser fields *Phys. Rev.* A **49** 2117

[16] Baltuška A *et al* 2003 Attosecond control of electronic processes by intense light fields *Nature* **421** 611

[17] Goulielmakis E, Yakovlev V S, Cavalieri A L, Uiberacker M, Pervak V, Apolonski A, Kienberger R, Kleineberg U and Krausz F 2007 Attosecond control and measurement: lightwave electronics *Science* **317** 769

[18] Eckle P *et al* 2008 Attosecond ionization and tunneling delay time measurements in helium *Science* **322** 1525

[19] Ammosov M V, Delone N B and Krainov V P 1986 Tunnel ionization of complex atoms and of atomic ions in an alternating electromagnetic field *Sov. Phys.—JETP* **64** 1191

[20] Corkum P B, Burnett N H and Ivanov M Y 1994 Subfemtosecond pulses *Opt. Lett.* **19** 1870

[21] Ivanov M, Corkum P B, Zuo T and Bandrauk A 1995 Routes to control of intense-field atomic polarizability *Phys. Rev. Lett.* **74** 2933

[22] Li P-C, Zhou X-X, Wang G-L and Zhao Z 2009 Isolated sub-30-as pulse generation of an He^+ ion by an intense few-cycle chirped laser and its high-order harmonic pulses *Phys. Rev.* A **80** 053825

[23] Mashiko H *et al* 2008 Double optical gating of high-order harmonic generation with carrier-envelope phase stabilized lasers *Phys. Rev. Lett.* **100** 103906

[24] Feng X, Gilbertson S, Mashiko H, Wang H, Khan S, Chini M, Wu Y, Zhao K and Chang Z 2009 Generation of isolated attosecond pulses with 20 to 28 femtosecond lasers *Phys. Rev. Lett.* **103** 183901

[25] Gauthey F I, Keitel C H, Knight P L and Maquet A 1995 Role of initial coherence in the generation of harmonics and sidebands from a strongly driven two-level atom *Phys. Rev.* A **52** 525

[26] Ishikawa K 2003 Photoemission and ionization of He^+ under simultaneous irradiation of fundamental laser and high-order harmonic pulses *Phys. Rev. Lett.* **91** 043002

[27] Emelin M Y, Ryabikin M Y and Sergeev A M 2005 Emission of an extremely short light pulse by an electron wavepacket detached from an excited atom *Laser Phys.* **15** 903

[28] Sanpera A, Watson J B, Lewenstein M and Burnett K 1996 Harmonic-generation control *Phys. Rev.* A **54** 4320

[29] Wang B, Cheng T-W, Li X-F and Fu P 2004 High-harmonic generation by initial coherent states in a short laser pulses *Chin. Phys. Lett.* **21** 1727

[30] Zhao J and Zhao Z 2008 Probing H_2^+ vibrational motions with high-order harmonic generation *Phys. Rev.* A **78** 053414

[31] Watson J B, Sanpera A, Chen X and Burnett K 1996 Harmonic generation from a coherent superposition of states *Phys. Rev.* A **53** R1962

[32] Averbukh V 2004 High-order harmonic generation by excited helium: the atomic polarization effect *Phys. Rev.* A **69** 043406

[33] Wernet Ph *et al* 2009 Real-time evolution of the valence electronic structure in a dissociating molecule *Phys. Rev. Lett.* **103** 013001

[34] Gräfe S, Engel V and Ivanov M Y 2008 Attosecond photoelectron spectroscopy of electron tunneling in a dissociating hydrogen molecular ion *Phys. Rev. Lett.* **101** 103001

[35] Seideman T, Ivanov M Yu and Corkum P B 1995 Role of electron localization in intense-field molecular ionization *Phys. Rev. Lett.* **75** 2819

[36] Zuo T and Bandrauk A D 1995 Charge-resonance-enhanced ionization of diatomic molecular ions by intense lasers *Phys. Rev.* A **52** R2511

[37] Chelkowski S, Yudin G L and Bandrauk A D 2006 Observing electron motion in molecules *J. Phys. B: At. Mol. Opt. Phys.* **39** S409

[38] Yudin G L, Chelkowski S, Itatani J, Bandrauk A D and Corkum P B 2005 Attosecond photoionization of coherently coupled electronic states *Phys. Rev.* A **72** 051401

[39] Singh K P *et al* 2010 Control of electron localization in deuterium molecular ions using attosecond pulse train and a many cycle infrared pulse *Phys. Rev. Lett.* **104** 023001

[40] Kling M F *et al* 2006 Control of electron localization in molecular dissociation *Science* **312** 246

[41] Tong X M and Lin C D 2007 Dynamics of light-field control of molecular dissociation at the few-cycle limit *Phys. Rev. Lett.* **98** 123002

[42] He F, Ruiz C and Becker A 2007 Control of electron excitation and localization in the dissociation of H_2^+ and its isotopes using two sequential ultrashort laser pulses *Phys. Rev. Lett.* **99** 083002

[43] Wörner H J, Bertrand J B, Kartashov D V, Corkum P B and Villeneuve D M 2010 Following a chemical reaction using high-harmonic interferometry *Nature* **466** 604

[44] Wörner H J, Bertrand J B, Corkum P B and Villeneuve D M 2010 High-harmonic homodyne detection of the ultrafast dissociation of Br2 molecules *Phys. Rev. Lett.* **105** 103002

[45] Lein M, Hay N, Velotta R, Marangos J P and Knight P L 2002 Interference effects in high-order harmonic generation with molecules *Phys. Rev.* A **66** 023805

[46] Strelkov V 2010 Role of autoionizing state in resonant high-order harmonic generation and attosecond pulse production *Phys. Rev. Lett.* **104** 123901

[47] Bian X B and Bandrauk A D 2011 Phase control of multichannel molecular high-order harmonic generation by the asymmetric diatomic molecule HeH_2^+ in two-color laser fields *Phys. Rev.* A **83** 023414

[48] Mairesse Y *et al* 2003 Attosecond synchronization of high-harmonic soft x-rays *Science* **302** 1540

[49] Kazamias S and Balcou Ph 2004 Intrinsic chirp of attosecond pulses: single-atom model versus experiment *Phys. Rev.* A **69** 063416

[50] Kanai T, Takahashi E J, Nabekawa Y and Midorikawa K 2007 Destructive interference during high harmonic generation in mixed gases *Phys. Rev. Lett.* **98** 153904

[51] Dinu L C, Muller H G, Kazamias S, Mullot G, Augé F, Balcou Ph, Paul P M, Kovačev M, Breger P and Agostini P 2003 Measurement of the subcycle timing of attosecond XUV bursts in high-harmonic generation *Phys. Rev. Lett.* **91** 063901

[52] Smirnova O, Mairesse Y, Patchkovskii S, Dudovich N, Villenenve D, Corkum P and Ivanov Yu 2009 High harmonic interferometry of multi-electron dynamics in molecules *Nature* **460** 972